atmosphere

Article

Positive Effect Observed on Reducing Criteria Pollutant Emissions Provided by Provisional Local Regulations during the 2022 Winter Olympics

Zongwen Shi [1], Zhoupeng Ren [2,*], Junfu Fan [1,2,*], Jiwei Zuo [1], Yu Gao [1] and Fulu Wei [3]

1 School of Civil Engineering and Geomatics, Shandong University of Technology, Zibo 255000, China; 21407010766@stumail.sdut.edu.cn (Z.S.); 21407010773@stumail.sdut.edu.cn (J.Z.); 21507020775@stumail.sdut.edu.cn (Y.G.)
2 State Key Laboratory of Resources and Environmental Information System, Institute of Geographic Sciences and Natural Resources Research, Chinese Academy of Sciences, Beijing 100101, China
3 School of Transportation and Vehicle Engineering, Shandong University of Technology, Zibo 255000, China; weifulu@sdut.edu.cn
* Correspondence: renzp@lreis.ac.cn (Z.R.); fanjf@lreis.ac.cn (J.F.); Tel.: +86-177-0105-7289 (Z.R.); +86-153-0533-0963 (J.F.)

Abstract: This study examined the impact of temporary air quality control measures on reducing pollutants during the 2022 Winter Olympics in China, utilizing real-time monitoring data from 2017 and 2022 to assess spatial and temporal variations in critical air pollutant concentrations. The results showed that concentrations of $PM_{2.5}$, PM_{10}, CO, SO_2, and NO_2 in the Beijing–Tianjin–Hebei region during the Olympic Games showed a marked decrease compared to the historical period, with reductions of 36.59%, 20.35%, 33.95%, 28.90%, and 22.70%, respectively. Significant north–south spatial differences were observed in Beijing, Tianjin, and Hebei Province during the Olympic period. The cities of Zhangjiakou, Chengde, Qinhuangdao, Beijing, and Tangshan showed the most significant pollution reduction. Based on assessments conducted during the Olympic period, it was noted that more than 95% of the daily average concentrations of pollutants are below the maximum values set by the World Health Organization for the interim target. Our research shows that provisional regulations effectively control the emission of air pollutants, providing a solid reference and basis for ensuring air quality during major international events.

Keywords: 2022 Winter Olympics; air pollutants; particulate matter; influencing factor; combined indicators; pollution control effectiveness

Citation: Shi, Z.; Ren, Z.; Fan, J.; Zuo, J.; Gao, Y.; Wei, F. Positive Effect Observed on Reducing Criteria Pollutant Emissions Provided by Provisional Local Regulations during the 2022 Winter Olympics. *Atmosphere* **2023**, *14*, 1774. https://doi.org/10.3390/atmos14121774

Academic Editor: Klaus Schäfer

Received: 11 October 2023
Revised: 4 November 2023
Accepted: 28 November 2023
Published: 30 November 2023

1. Introduction

The concentrations of criteria air pollutants (suspended particulate matter (PM) with a diameter less than or equal to 2.5 µm ($PM_{2.5}$), PM_{10}, SO_2, NO_2, CO, and O_3) are the most commonly used indicators of the air pollution degree. Among them, the concentration of suspended PM in the air is correlated with mortality related to cardiopulmonary diseases [1–3]. Industrial fossil fuel combustion and air pollutants, including SO_2, NO_2, and CO, in vehicle exhaust emissions are among the most important factors contributing to increased human respiratory and cardiovascular system morbidity [4–6]. Ozone in the atmospheric stratosphere plays a crucial role in blocking harmful solar ultraviolet (UV) rays, but ozone (considered a secondary pollutant) in the surface atmosphere can greatly irritate the human respiratory system [4,7]. Ozone in the surface atmosphere is mainly produced via photochemical reactions, and the production rate is influenced by a combination of organic chemicals, nitrogen oxides, and sunlight [4,8,9]. Its concentration can also reflect the air pollution degree. Thus, it is obvious that the study of the concentration changes of criteria air pollutants is very important for human health, economy, society, and sustainable development.

Anthropogenic activities notably influence air quality. Disease containment, industrial production, and traditional customs have all been demonstrated to rapidly affect regional air quality. Tao et al. found that prevention measures to control the spread of coronavirus disease 2019 (COVID-19) by reducing vehicle movement and factory production levels could improve air quality [10]. Wang et al. reported that prohibiting fireworks during the Lunar New Year in Shanghai, China could effectively reduce the $PM_{2.5}$ concentration [11,12]. The Olympic Games are a global sporting event, and the air quality conditions in the host area directly affect the physical health and competitive level of athletes [13]. The International Olympic Committee (IOC) requires the continuous monitoring of air pollutant concentrations at host venues to ensure that the air quality reaches relevant standards [14]. The Metro Atlanta Rapid Transit Authority reduced traffic emissions and safeguarded the air quality during the 1996 Atlanta Olympics by using a 24 h traffic management system and increasing public transportation services. The city of Atlanta lowered its average daily emissions of CO, NO_2, and PM_{10} by 18.5%, 6.8%, and 16.1%, respectively [15]. During the Beijing Summer Olympics in 2008, the Chinese government enacted the Measures to Safeguard the Air Quality in Beijing for the Games of the 29th Olympics, which focused on reducing soot emissions originating from the power industry and PM emissions. Beijing exhibited a 90% reduction in PM_{10} emissions originating from the construction sector and a 35% reduction in the total emissions based on an air pollution prediction model [16]. The Nanjing Municipal Government implemented the Nanjing Temporary Environmental Regulations for Air during the 2014 Youth Olympic Games, which attempted to reduce air pollution through a series of prevention and control measures, such as closing coal-fired plants, shutting down construction, and increasing public transportation. Subsequent remote sensing observations revealed that the NO_x concentration was approximately 25% lower than the average concentration from 2005 to 2012, and the implementation of the above regulation effectively improved the regional air quality [17]. The 24th Winter Olympic Games were held in Beijing and Zhangjiakou, China. The Chinese government acted to ensure the regional air quality. Moreover, specific air quality targets were established in 64 cities to reduce the concentrations of harmful microscopic particles ($PM_{2.5}$), dozens of factories in the Beijing–Tianjin–Hebei (BTH) region were temporarily closed [18], and the number of severe pollution days from October 2021 to March 2022 was greatly reduced. During the 24th Winter Olympic Games readiness period, Wang et al. (2022) predicted, through a combination of atmospheric circulation and climate prediction models, that the emissions of SO_2, NO_2, CO, and other pollutants would follow a downward trend [19]. Chu et al. assessed the trends of $PM_{2.5}$, PM_{10}, SO_2, and NO_2 air quality in Beijing and Zhangjiakou before and after the 2022 Winter Olympics using ground-based monitoring data. Furthermore, it found that air pollutants decreased significantly during the Winter Olympics [20]. Similarly, Wu et al. found a significant decrease in $PM_{2.5}$ concentrations and an increase in air quality during the Olympic Games [21].

We analyzed—by combining past research with continuous observation of the concentrations of criteria—pollutants in the Beijing–Tianjin–Hebei region over various subperiods. We further analyzed the spatial and temporal variations of the concentrations of criteria pollutants and compared them with historical levels over the same period, and assessed whether the interim air pollution control policies and regulations were effective and to what extent these measures improved air quality during the Winter Olympics in the Olympic Games host regions (Beijing and Zhangjiakou). This research can be a reliable reference point for ensuring air quality during significant international events. It can contribute to regional environmental decision making, economic development, social governance, and sustainable urban development.

2. Materials and Methods

2.1. Air Pollution Prevention Policies and Regulations

To safeguard air quality during the 24th Winter Olympic Games and the 13th Winter Paralympic Games (hereinafter referred to as the 2022 Winter Olympics), appropriate departments have released applicable measures (Table 1). The Ministry of Industry and Information Technology and the Ministry of Ecology and Environment of China issued the policy regulation Notification of the Two Departments on BTH Region 2021–2022 Heating Season Steel Industry Staggered Production on 30 September 2021. The provisions of this law, developed from 15 November 2021 to 15 March 2022, required heavy industry enterprises in Beijing, Tianjin, Hebei, Shanxi, Shandong, and Henan provinces to reduce their criteria air pollutant emissions [22]; moreover, heavy industries and high-emission enterprises in Shijiazhuang, Tangshan, Xingtai, Handan, Langfang, Qinhuangdao, and Cangzhou were prohibited from engaging in production activities. Moreover, the General Office of the Tianjin Municipal People's Government issued the Notice of Firework Inhibition During the Spring Festival in 2022 to ensure the safe and smooth progression of the Winter Olympics, which prohibited the public from lighting fireworks during the Lunar New Year to prevent air pollution [23]. The control measures implemented in Beijing were particularly strict. The Beijing Municipal People's Government issued the Notice on Temporary Traffic Management Measures during the Olympic Cycle, which imposed strict traffic controls from January to 15 March 2022. These controls included the creation of dedicated Olympic lanes, restrictions on foreign vehicles, and a ban on medium and heavy fuel (gas) trucks [24].

Table 1. Air control measures during the 2022 Winter Olympic Games.

Agency	Period	Regulations	Impact Area
Ministry of Industry and Information Technology Ministry of Ecology and Environment	15 November 2021–15 March 2022	Heavy industrial enterprises should aim to reduce air pollutant emissions to achieve staggered production and pollutant reduction	Beijing, Tianjin, Hebei, Shanxi, Shandong, and Henan provinces
	1 January 2022–15 March 2022	High-emission enterprises were prohibited from engaging in production activities	Shijiazhuang, Tangshan, Xingtai, Handan, Langfang, Qinhuangdao, and Cangzhou in Hebei Province
Tianjin Municipal Government	1 January 2022–15 March 2022	The discharge of fireworks was prohibited	Tianjin
Beijing Municipal Government	1 January 2022–15 March 2022	Vehicle restrictions were enacted, dedicated lanes were opened, and heavy fuel (gas) trucks were not allowed to drive on roads	Beijing

2.2. *Study Area and Air Monitoring Sites*

The 2022 Winter Olympics were held in the BTH region of China (Figure 1), encompassing the cities of Beijing and Zhangjiakou, which exhibit a high topography in the northwest and low plains in the southeast, as well as low mountains and coastal wetlands. The Yanshan Mountains, Taihang Mountains, and Bohai Sea surround the region, creating a unique geomorphological environment. The region belongs to a temperate semihumid and semiarid continental monsoon climate zone with high summer rainfall levels and distinct dry and wet seasons [25,26]. These geographical and climatic characteristics provide favorable conditions for hosting the 2022 Winter Olympics. The BTH region includes 11 prefecture-level cities in Beijing (BJ), Tianjin (TJ), and Hebei (HB) provinces, including Shijia-zhuang (SZJ), Tangshan (TS), Qinhuangdao (QHD), Handan (HD), Xingtai (XT), Langfang (LF), Baoding (BD), Hengshui (HS), Zhangjiakou (ZJK), Chengde (CD), and Cangzhou (CZ). The BTH region has become one of the most economically developed regions in China, with a suitable industrial base and political and economic advantages, but it is also one of the most seriously affected regions in China in terms of air pollutant emissions [26–29].

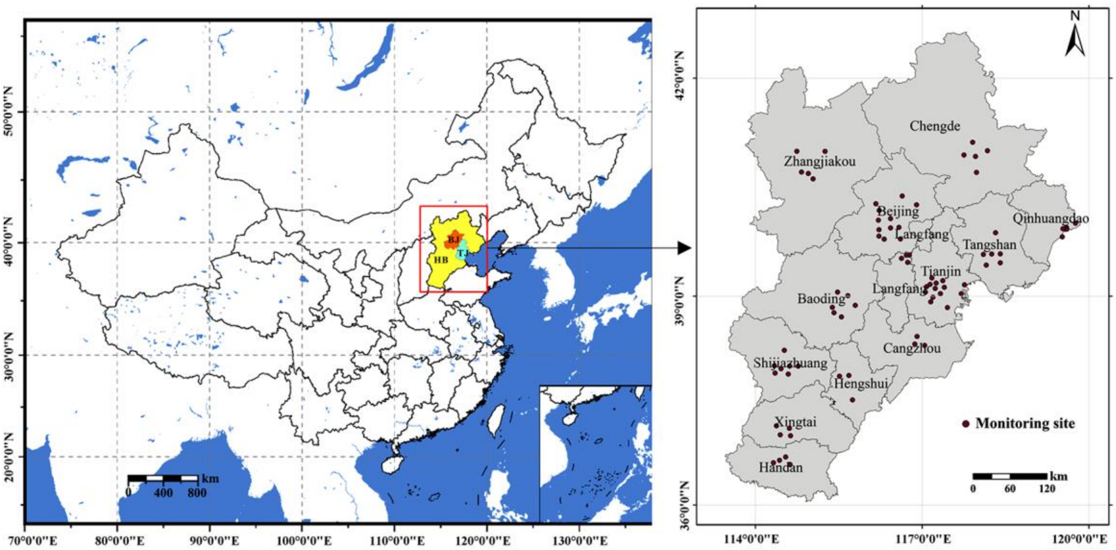

Figure 1. Study area and air monitoring site distribution.

We obtained hourly monitoring data from 78 ground air quality monitoring sites of the air quality monitoring network of the China Environmental Monitoring Center (http://www.cnemc.cn accessed on 10 January 2023) for the period of 1 December 2017 to 19 July 2022 (Figure 1). The data include monitoring data of the criteria air pollutants $PM_{2.5}$, PM_{10}, SO_2, NO_2, O_3 (concentration in $\mu g/m^3$), and CO (concentration in mg/m^3), as well as Air Quality Index (AQI) data and monitoring station information such as the station code, city, and latitude and longitude accession numbers.

2.3. Definition of the Time Window

The earliest date for the promulgation of air pollution prevention policies and regulations for the 2022 Winter Olympics was 15 November 2021 (Table 1). The opening date of the Winter Olympics was 4 February, and the end date of the enacted air pollution prevention policies and regulations was 15 March, which is the main basis for our time window delineation. Therefore, we defined the period of 1 December 2021 to 4 February 2022 as the pre-Olympic subperiod (Pre-O period), totaling 65 days; the period of 4 February 2022 to 15 March 2022 was defined as the Olympic subperiod (O period), totaling 40 days; and the 65-day period after 15 March 2022 was defined as the post-Olympic subperiod (Post-O period), totaling 65 days. Moreover, 19 May 2022 was defined as the end date of the Olympic cycle. In addition, to ensure the consistency of the comparison of air pollutant concentrations, historical monthly intervals covering the above four time periods were used in this paper as historical periods (1 December 2017–19 July 2021). It should be noted that the time period of 1 December 2019 to 19 July 2020 was excluded from the considered historical periods in this paper due to the significant reduction in air pollutants during the COVID-19 lockdown in China [30–33]. In addition, we defined the 60-day period of 19 May to 19 July 2022 as the beyond-Olympic cycle period (Beyond-O period), thus eliminating the impacts of the various control policies implemented during the Winter Olympics and ensuring the comparison to the various Olympic cycle subperiods to reveal the emission-reduction effect (Figure 2). The study time window division scheme is summarized below.

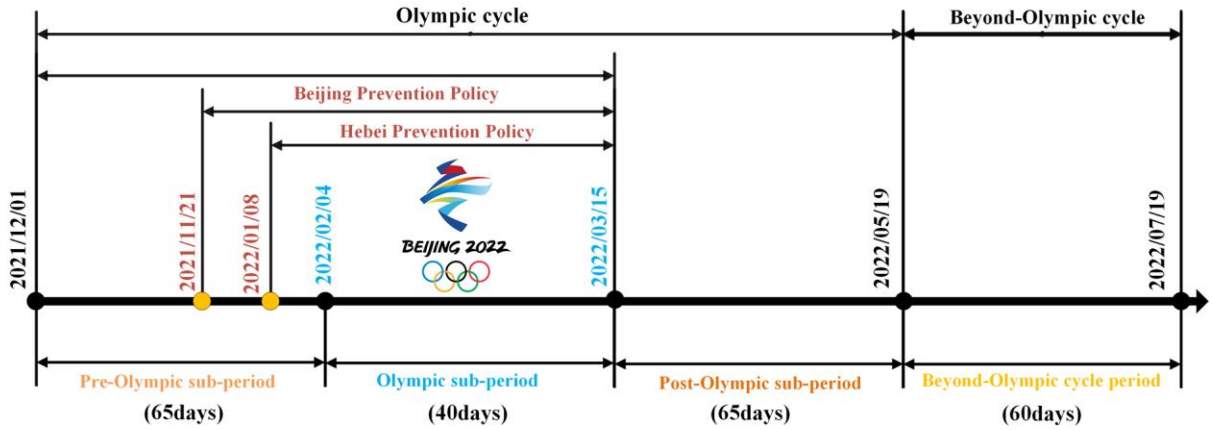

Figure 2. Time window and timing of policy implementation.

2.4. Air Pollutant Dataset

We preprocessed the hourly observation data obtained from 1 December 2017 to 19 July 2022 to generate a standard air pollutant dataset, as shown in Figure 3, to ensure temporal continuity and to relate the observation data to the geographic site locations. We correlated the data items with the corresponding geographic locations based on the latitude and longitude attributes of each monitoring site. Statistically, in the dataset, pollutant monitoring values were missing during different time periods or at various stations to different degrees, and the number of missing values accounted for approximately 3% of the total data.

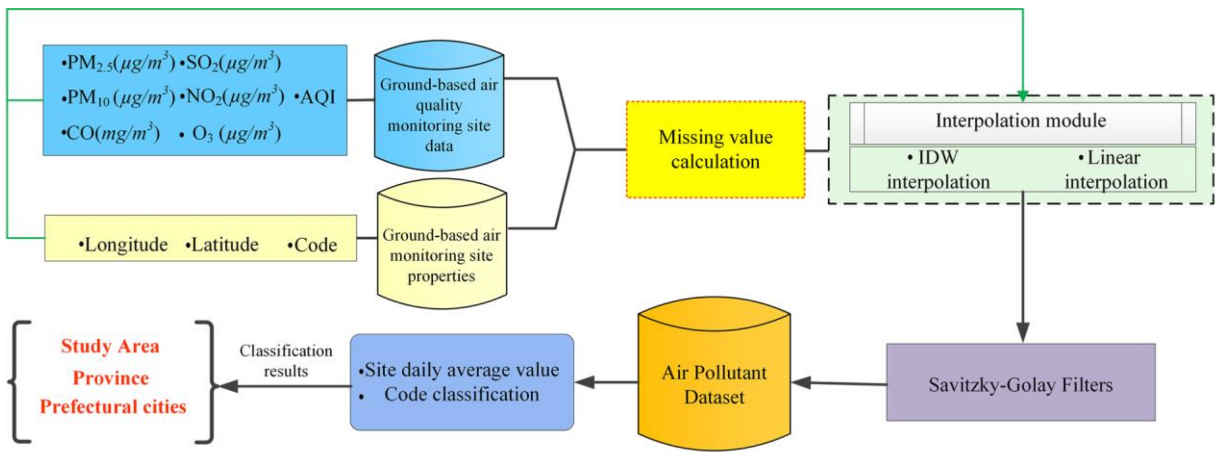

Figure 3. Air dataset production process.

Regarding the missing hourly pollutant concentration values in the dataset, we used two interpolation methods for replacement purposes. First, if there were missing values in the dataset at a single monitoring station within the same city, with complete data at n surrounding stations, we calculated the distance to the surrounding stations and interpolated the missing data using the inverse distance weighting method (Equations (1) and (2)) [34]. Second, if there were missing data at multiple sites around the same city and the inverse distance weighting interpolation conditions could not be satisfied, we then interpolated the missing values using the time series linear interpolation method based on the data retrieved from individual sites. With the use of these methods, we could achieve the interpolation and supplementation of missing data to generate a continuous and complete time series dataset. Furthermore, the continuous time series data for each site were processed using the Savitzky–Golay filter. This filter could improve the autocorrelation of the data and enhance the pollutant concentration trend over time, thus reducing noise and errors in the observed dataset [35]. The Savitzky–Golay filter could improve the autocorrelation and fluctuation of the data and enhance the pollutant concentration trend over time, thus reducing noise and errors in the observed dataset [35,36]. The application of inverse distance weighting for interpolation can consider the spatial correlation of monitoring stations [37].

$$Z_o = \sum_{i=1}^{n} \frac{1}{(D_i)^p} z_i \left(\sum_{i=1}^{n} \frac{1}{(D_i)^p} \right)^{-1} \tag{1}$$

$$D_i = \sqrt{(x_o - x_i)^2 + (y_o - y_i)^2} \tag{2}$$

where Z_0 denotes the missing value at a given monitoring station, Z_i is the pollutant monitoring value at i sample stations (i = 1, 2, 3…n), p is the power exponent of the distance, D_i is the distance to each neighboring station, and x and y are the location information attributes of the stations.

2.5. Reducing the Impacts of Weather and Human Factors on the Dataset

Notable impacts of extreme weather events and anthropogenic activities on the air quality have been widely noted. For example, hazy weather can lead to the accumulation and stagnation of airborne PM; dust storms and tornadoes may transport surface PM into the air, resulting in a sharp and rapid increase in airborne PM concentrations; and hot weather can lead to increased emissions of pollutants such as volatile organic compounds (VOCs) and nitrogen oxides (NO_x), resulting in further increases in ozone (O_3) concentrations [38–44]. In addition, anthropogenic activities such as fires, traffic congestion, COVID-19 lockdown measures, and industrial production activities can release large amounts of air pollutants within a short period of time. Fossil fuel combustion leads to short-term increases in O_3 and particulate matter concentrations in the region, leading to heavy metal pollution and subsequent human disease [45,46]; emissions from industry, forest fires, and domestic activities lead to increases in SO_2, PM_{10}, and VOCs emissions, threatening human life and health [47,48]. The COVID-19 mitigation measure leads to a decrease in particulate matter concentrations, a significant reduction in aerosols, and an improvement in air quality [31,49]. This shows that anthropogenic activities have a significant impact on air quality.

These extreme climatic events and anthropogenic activities may cause extreme values, which may affect the overall criteria pollutant concentrations within a given time window. Thus, meteorological factors and anthropogenic activities can greatly impact the air quality.

To manage these inevitable extreme values, a density-based local outlier factor (LOF) method was used to detect and reject outliers in the dataset. This method can be effectively applied to a continuous time-based observation dataset, independent of the data distribution, and can significantly improve the outlier detection rate and reduce the time complexity of anomaly detection [50–53].

First, we expanded the hourly observations at the various sites and calculated the reachable distance of data point P $reach\_dist_k(o,p)$ based on the data density around the data point (Equation (3)):

$$reach - dist_k(o,p) = \max\{d_k(o), d(o,p)\} \tag{3}$$

where $d(o,p)$ is the distance from the observed data point P to another observed data point O; $reach - dist_k(o,p)$ is the kth reachable distance from data point O to data point P, defined as the larger of $d_k(o)$ and $d(o,p)$; and $d_k(o)$ is the kth reachable distance from data point O to data point P.

Second, we calculated the local reachability density of data point P $lrd_k(p)$ as follows (Equation (4)):

$$lrd_k(p) = \left(\frac{\sum_{O \in N_k(P)} reach - dist_k(o, p)}{|N_k(p)|} \right)^{-1} \quad (4)$$

where $lrd_k(p)$ is the local reachability density; $N_k(p)$ is the kth distance neighborhood of data point P, which is the set of points within the kth distance of index data point P; and $lrd_k(p)$ characterizes the density of data point P.

Finally, the local outlier factor $LOF_k(p)$ of data point P was calculated according to $lrd_k(p)$ and $N_k(p)$, the extreme value points of the dataset were eliminated according to the threshold of $LOF_k(p)$ (Equation (5)), and linear interpolation was applied to replace the missing points of the dataset after elimination, thus completing the air dataset production process.

$$LOF_k(p) = \frac{\sum_{O \in N_k(P)} \frac{lrd_k(o)}{lrd_k(p)}}{|N_k(p)|} = \frac{\sum_{O \in N_k(P)} lrd_k(o)}{|N_k(p)|} / lrd_k(p) \quad (5)$$

where $LOF_k(p)$ is the local outlier factor of data point P. The average local reachable density of the points in the neighborhood of point P $N_k(p)$ was compared to the local reachable density of point P. $LOF_k(p) \geq 1$ indicates that the density of point P is lower than that of its surrounding points, and point P is probably an outlier. $LOF_k(p) < 1$ indicates that the density of point P is higher than that of its surrounding points, and point P is very likely a normal point.

2.6. Statistical Analysis Methods

We classified the study regions, municipalities, provinces, and cities based on the geographical information of the monitoring sites and comprehensively analyzed the spatial and temporal characteristics of the criteria air pollutant concentrations during all four periods of the Olympic cycle (Pre-O, O, Post-O, and Beyond-O). To mitigate the effects of seasonal differences on the quantitative analysis of pollutants, we controlled for time interval variables to ensure that both the historical and current pollutant concentrations were subject to the same seasonal interval [54–58]. To address the potential impact of continued regulatory control due to air quality policies implemented by governments [59], we used Levene's test to perform chi-square and two-sample *t* tests for the comparison of the differences in pollutant concentration data between the historical and current time periods [60–62]. At a significance level of 0.05, we used the *p* value (*p*) to determine the statistical significance of the correlation between the two samples. The null hypothesis H_0 indicates that the pollutant concentrations do not significantly differ between the historical and selected time interval samples, while the alternative hypothesis H_1 indicates that the pollutant concentrations of the historical sample significantly differ from those of the selected time interval sample. H_1 is accepted for $p < 0.05$, and H_0 cannot be rejected for $p > 0.05$. Hypothesis testing of the historical and current samples during the Beyond-O period can verify the impact of historical trends.

Thereafter, we calculated the median and mean values of the air pollutant concentrations at each scale during the different periods and combined the spatial and temporal division categories to compare the pollutant concentrations in the study area on each scale to those during the historical period. We used the median of the time series data during each period as an indicator to measure the changes in pollutant concentrations throughout the Olympic cycle and during the historical period via sample hypothesis testing to reduce the effects of extreme observations. In addition, the absolute values and percentages of the changes in the different categories of pollutants were calculated (Equation (6)), and the hypothesis test results were summarized and analyzed.

$$R_{change} = \frac{V_{current} - V_{history}}{V_{history}} \times 100\% \quad (6)$$

where R_{change} is the percentage change of the pollutants over the historical period relative to the different time periods selected in this study, $V_{history}$ is the median value of the sample over the historical period, and $V_{current}$ is the median value over the different time periods selected in this study.

3. Results and Discussion

3.1. Analysis of the Criteria Pollutant Concentrations in the Entire Study Area, Provinces, and Municipalities within a Given Time Window

We statistically analyzed the concentration changes of criteria air pollutants ($PM_{2.5}$, PM_{10}, SO_2, CO, and O_3NO_2) in the BTH region, including BJ, TJ, and HB, within different time intervals, aiming to clarify the effects of emission-reduction measures on the concentrations of various pollutants during the different time periods and in the major regions (Figure 4).

3.1.1. Overall Evaluation Analysis of $PM_{2.5}$

Figure 4a shows the daily average $PM_{2.5}$ concentration statistics for the BTH region, including BJ, TJ, and HB, over the four time intervals (Pre-O, O, Post-O, and Beyond-O) relative to the historical period. Specific statistics (numerical values) are detailed in Table 2. The statistical results showed that the $PM_{2.5}$ concentrations in all parts of the BTH region during the O period highly significantly differed from those during the historical period, in which the $PM_{2.5}$ concentration in the whole BTH region decreased by 36.59%, while the ratios of decrease in the $PM_{2.5}$ concentrations in Beijing, Tianjin, and Hebei were 46.07%, 38.54%, and 35.78%, respectively. Beijing contributed the most to the observed $PM_{2.5}$ emission reduction percentage during the O period.

Table 2. Statistical values, change rates, and hypothesis test results for the $PM_{2.5}$ concentration (μg/m^3) during the different time periods in the BTH, BJ, TJ, and HB regions based on the historical and current data.

Region	Period	Historical Median	Current Median	Absolute Change	Change Rate	*p* Value
BTH	Pre-O	45.94	44.63	−1.30	−2.84%	0.652
	O **	53.17	33.72	−19.45	−36.59%	0.000
	Post-O *	38.75	32.38	−6.37	−16.45%	0.022
	Beyond-O	23.78	21.70	−2.07	−8.73%	0.257
BJ	Pre-O	25.33	26.91	1.57	6.21%	0.767
	O **	45.68	24.63	−21.05	−46.07%	0.000
	Post-O	34.83	28.81	−6.02	−17.29%	0.121
	Beyond-O	16.85	19.38	2.53	15.02%	0.134
TJ	Pre-O	45.39	44.57	−0.81	−1.79%	0.317
	O **	61.55	37.83	−23.72	−38.54%	0.002
	Post-O *	37.06	33.06	−4.00	−10.79%	0.028
	Beyond-O	24.38	23.43	−0.94	−3.87%	0.421
HB	Pre-O	50.21	48.84	−1.38	−2.74%	0.821
	O **	55.24	35.48	−19.76	−35.78%	0.001
	Post-O *	38.66	32.77	−5.89	−15.23%	0.026
	Beyond-O	25.19	21.29	−3.90	−15.47%	0.057

*: If $p < 0.05$, the sample is significantly different; **: if $p < 0.01$, the sample is highly significantly different.

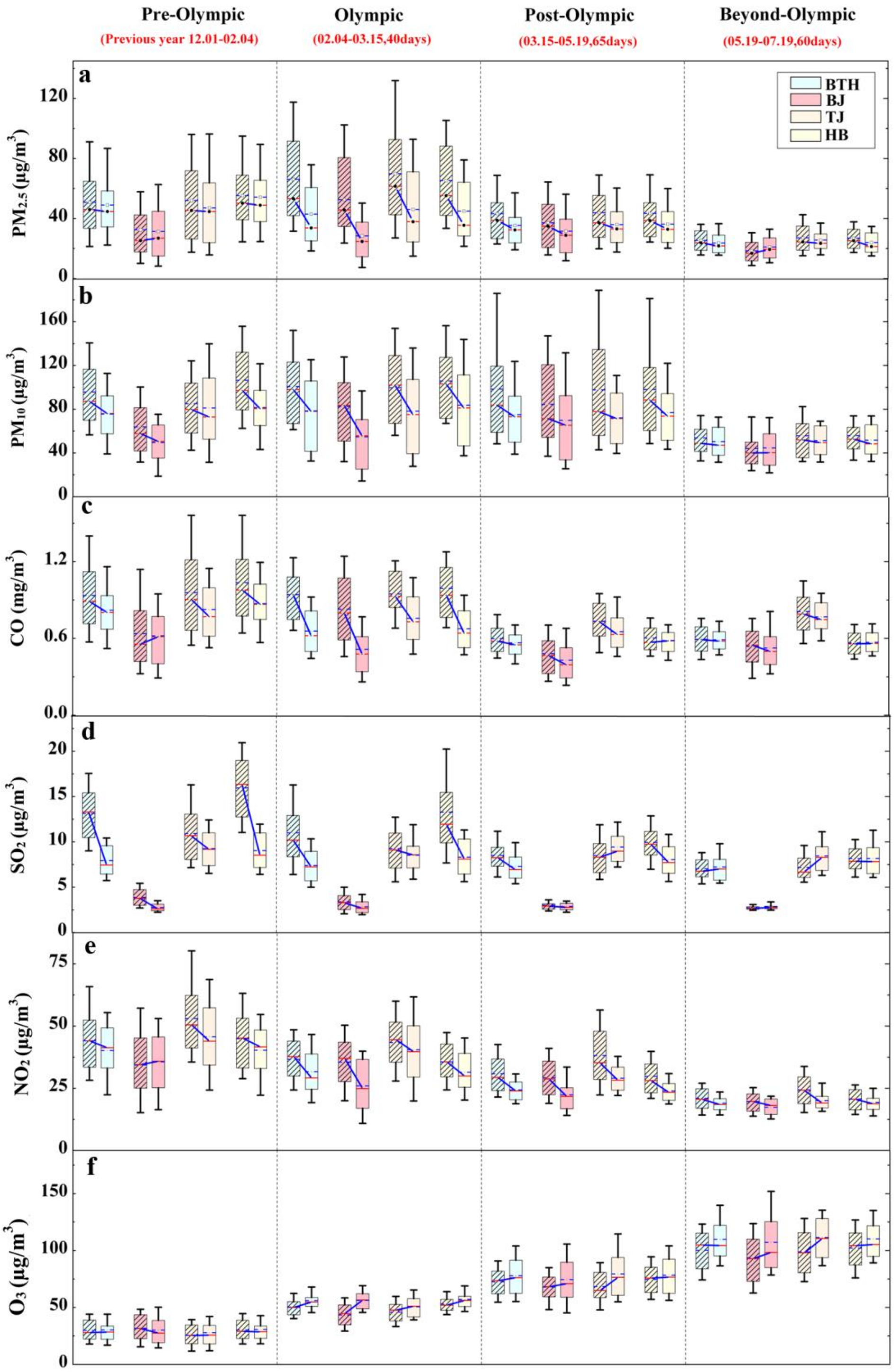

Figure 4. Subfigures (**a**–**f**) show the daily average criteria pollutants concentrations ($PM_{2.5}$, PM_{10}, SO_2, CO, NO_2, and O_3) in the BTH region, including BJ, TJ, and HB, within each time interval between the historical and current periods. The solid red horizontal line indicates the median pollutant concentration within the time interval; the dashed blue horizontal line indicates the mean pollutant concentration within the time interval; the top and bottom of the box indicate the 75th and 25th percentile ranges, respectively; the top and bottom whiskers indicate the 95th and 5th percentile values, respectively; and the divergence indicates the deviation. Solid line-filled boxes with solid colors represent History, whereas solid-colored filled boxes represent Current. The slope of the line represents a negative proxy for decline, the slope of the line represents a positive proxy for increase, and the slope of the line tends towards zero, indicating no change.

Moreover, we found that there was no significant difference in the $PM_{2.5}$ concentration in each part of the BTH region between the Pre-O and historical periods. However, during the Post-O period, significant differences were found in the $PM_{2.5}$ concentrations in the BTH, TJ, and HB regions, while during the Beyond-O period, none of the regions exhibited significant differences in pollutant concentrations, and it could be assumed that the pollutant concentrations returned to normal historical levels. Therefore, we could conclude that the implemented control measures reduced the $PM_{2.5}$ concentration during the Winter Olympics (O period).

The nonsignificant difference in the $PM_{2.5}$ concentration during the Post-O period may be a result of the lag effect of the combined emission reduction measures and meteorological conditions, which are usually lagged by precipitation and relative humidity, respectively, on the PM concentration [16,63]. Thereafter, as the lag effects of the abatement measures diminished, the pollutant concentrations returned to normal levels, with no significant differences relative to the historical periods. Thus, our study showed that in the BTH region, the control measures implemented during the Winter Olympics effectively reduced the $PM_{2.5}$ concentration. Beijing contributed the most to the obtained $PM_{2.5}$ emission reduction percentage in the process. Studies have shown that for Beijing, the local contribution was 62% and 69% in January and March, respectively, while the regional transport was mainly from the surrounding cities of Zhangjiakou, Baoding, and Langfang [64,65]. During the Olympic Games period (January to March), Hebei Province implemented control measures targeting industries, which reduced the input of PM emissions to Beijing. Therefore, PM emissions in Beijing during this period were mainly from local contributions, significantly affected by local control measures. The short-term traffic control measures may be one of the reasons for the sharp decrease in $PM_{2.5}$ concentrations in Beijing.

3.1.2. Overall Evaluation Analysis of PM_{10}

We statistically analyzed the PM_{10} concentration in the BTH region during the four periods of the current and historical years (Figure 4b and Table 3), and the results showed that the PM_{10} concentration significantly decreased during the Winter Olympics (O period), while there was no significant difference in the PM_{10} concentration between the Beyond-O and historical periods. Therefore, we could conclude that the emission-reduction measures implemented by the government successfully reduced the PM_{10} concentration during the Winter Olympics.

Table 3. Statistical values, change rates, and hypothesis test results for the PM_{10} concentration ($\mu g/m^3$) during the different time periods in the BTH, BJ, TJ, and HB regions based on the historical and current data.

Region	Period	Historical Median	Current Median	Absolute Change	Change Rate	*p* Value
BTH	Pre-O **	87.25	76.00	−11.26	−12.90%	0.001
	O *	98.01	78.06	−19.94	−20.35%	0.015
	Post-O **	83.74	73.09	−10.65	−12.71%	0.004
	Beyond-O	48.85	47.10	−1.75	−3.59%	0.315
BJ	Pre-O **	57.85	50.55	−7.30	−12.63%	0.003
	O **	83.51	55.72	−27.79	−33.27%	0.003
	Post-O	71.46	65.36	−6.09	−8.53%	0.059
	Beyond-O	40.02	40.24	0.22	0.54%	0.900
TJ	Pre-O	79.89	72.83	−7.06	−8.84%	0.551
	O *	102.05	75.10	−26.95	−26.41%	0.027
	Post-O **	77.86	71.49	−6.37	−8.18%	0.001
	Beyond-O	51.92	49.42	−2.50	−4.81%	0.249
HB	Pre-O **	97.24	80.53	−16.71	−17.18%	0.000
	O *	103.28	81.16	−22.11	−21.41%	0.014
	Post-O **	88.47	73.60	−14.87	−16.80%	0.005
	Beyond-O	52.67	48.32	−4.35	−8.26%	0.205

*: If $p < 0.05$, the sample is significantly different; **: if $p < 0.01$, the sample is highly significantly different.

During the O period, Beijing contributed the most to the emission reduction percentage effect, at 33.27%, followed by Tianjin and Hebei, at 26.41% and 21.41%, respectively. The PM_{10} concentration in Beijing decreased very significantly during this period, which may be due to the effect of the implemented traffic-restriction measures. We also found that the PM_{10} concentrations in Hebei and Beijing during the Pre-O period significantly differed from those during the historical periods, indicating that the government applied effective measures to control the PM_{10} concentration during the Pre-O period, which may be related to the in-plant emission-reduction measures in both regions during the Pre-O period. The PM_{10} concentration in Hebei Province also significantly differed from that in the other regions throughout the Olympic cycle, indicating that the longest cycle of control measures was implemented in Hebei Province.

Combining these analysis results, we could conclude that the PM_{10} concentration in the BTH region showed a more significant decrease during the O period, with a total percentage decrease of 20.35%. During this period, Beijing contributed the most to PM_{10} emission reduction, while Hebei Province implemented the longest control measure cycle. The PM_{10} concentration significantly decreased without a lag effect throughout the Olympic cycle, and when the lag effect of the control measures was eliminated, the pollutant concentrations returned to normal levels everywhere. This indicates that the government-issued emission-reduction measures achieved satisfactory results. Moreover, during the Beyond-O period, there were no significant deviations observed in PM_{10} concentrations in all three regions compared to the historical period. It can be concluded that the Olympic policy had an influence on the PM_{10} concentrations in the BTH area.

3.1.3. Overall Evaluation Analysis of CO

CO statistical analysis could facilitate the development of effective environmental policies and regulatory measures to reduce CO emissions and safeguard public health and environmental quality. Based on the statistical data (Figure 4c and Table 4), we found that during the O period, the CO concentration in the whole study area significantly decreased relative to the historical periods, with Beijing contributing the most, with a 40.15% reduction, followed by Hebei Province, with 31.61%, and Tianjin, with 21.46%. During the Beyond-O period, when Olympic factors were eliminated, there was no significant difference in the CO concentration in the study area relative to the historical periods, but the CO concentration in the BTH region was 33.95% lower during the O period than during the historical periods. Therefore, it could be concluded that the relevant air pollution prevention and control policies implemented during the Winter Olympics positively affected the CO emissions in the BTH region during the Beyond-O period.

We further observed that Hebei Province and Tianjin City achieved significant reductions in their CO concentrations during the Pre-O period, and according to the relevant reduction measures, the restriction of enterprise production activities during the Pre-O period played a key role in CO reduction [22]. Beijing, which is dominated by high-tech industries, has fewer emitting enterprises than the other two areas [29]; therefore, there was no significant reduction during the Pre-O period, while the traffic closure and control measures in Beijing during the O period could significantly reduce the CO concentrations. In conclusion, an unbalanced regional industrial structure often leads to variability in pollutant concentration changes.

During the Post-O period, the PM_{10} concentration in Tianjin continued to decrease, showing a highly significant difference, which indicates that Tianjin experienced a longer period of CO concentration control. In contrast, no significant differences in pollutant concentrations were observed in either Beijing or Hebei. Therefore, we could conclude that the BTH region achieved a significant reduction in the CO concentration during the Winter Olympics, with Beijing showing the highest percentage reduction and Tianjin adopting a longer CO concentration control cycle.

Table 4. Statistical values, change rates, and hypothesis test results for the CO concentration (mg/m^3) during the different time periods in the BTH, BJ, TJ, and HB regions based on the historical and current data.

Region	Period	Historical Median	Current Median	Absolute Change	Change Rate	*p* Value
BTH	Pre-O *	0.89	0.80	−0.09	−9.80%	0.017
	O **	0.94	0.62	−0.32	−33.95%	0.000
	Post-O	0.58	0.55	−0.03	−4.99%	0.152
	Beyond-O	0.59	0.58	−0.01	−2.05%	0.827
BJ	Pre-O	0.55	0.61	0.06	10.63%	0.724
	O **	0.80	0.48	−0.32	−40.15%	0.000
	Post-O	0.47	0.39	−0.07	−15.65%	0.119
	Beyond-O	0.55	0.50	−0.05	−8.99%	0.697
TJ	Pre-O *	0.90	0.77	−0.13	−14.89%	0.018
	O **	0.93	0.73	−0.20	−21.46%	0.000
	Post-O **	0.73	0.63	−0.10	−13.73%	0.005
	Beyond-O	0.79	0.75	−0.04	−5.57%	0.173
HB	Pre-O **	0.98	0.87	−0.11	−11.34%	0.001
	O **	0.94	0.64	−0.30	−31.61%	0.000
	Post-O	0.57	0.58	0.01	1.79%	0.375
	Beyond-O	0.56	0.56	0.00	0.71%	0.765

*: If $p < 0.05$, the sample is significantly different; **: if $p < 0.01$, the sample is highly significantly different.

3.1.4. Overall Evaluation Analysis of SO_2

Based on the data shown in Figure 4d and Table 5, it is evident that there is a significant difference in the concentration of SO_2 in the BTH area throughout the study period. Compared to those for $PM_{2.5}$, PM_{10}, and CO, the SO_2-reduction effect in the BTH region was the most obvious during the Pre-O period, with all three regions showing a highly significant reduction in the SO_2 concentration, with Hebei Province contributing the most, with a 47.82% reduction, followed by Beijing at 30.76% and Tianjin at 14.08%, which is consistent with the plant-reduction measures during the Pre-O period. During the O period, the SO_2 concentrations in both Beijing and Hebei Province showed significant decreases, with the abatement rate in Hebei Province reaching 32.15%, while the SO_2 concentration in Tianjin did not differ from that during the historical periods. During the Post-O period, the SO_2 concentration in Tianjin increased, while the SO_2 concentration in Beijing stabilized, and the SO_2 concentration in Hebei continued to show significant decreases, which may be related to the more concentrated industrial structure in Hebei. During the Beyond-O period, the SO_2 concentrations in Hebei and Beijing remained basically consistent with those during the historical periods, while Tianjin showed a highly significant increase.

Summarizing the above analysis results, we could conclude that Hebei Province achieved the greatest SO_2 emission reduction throughout the Olympic cycle and had the longest emission reduction period, which may be related to its concentrated industrial structure. Beijing also effectively reduced its SO_2 emissions during the Pre-O and O periods, while Tianjin only realized effective control during the Pre-O period, and the control effect during the O period was not significant. In general, the air pollution prevention and control policies in the Beijing, Tianjin, and Hebei regions played a positive role in lowering SO_2 emissions.

3.1.5. Overall Evaluation Analysis of NO_2 and O_3

NO_2 is a harmful gas usually part of the combustion emissions of nitrogen oxides stemming from fossil fuels [66]. NO_2 participates in photochemical reactions and interplays with other pollutants, ultimately leading to the generation of O_3 [67]. O_3 poses a grave threat to human respiratory health and air quality [68]. According to Figure 4f and Table 6, we can find that the NO_2 concentration in TJ decreased by 13.42% compared with the historical period in the Pre-O period, followed by a decrease of 7.86% in HB, and there was no significant decrease in the NO_2 concentration in BJ. It is worth noting that the decreases in NO_2 concentrations in TJ and HB Province during the Pre-O period may be related to industry emission-reduction measures. The NO_2 concentration in BJ decreased by 32.74% during the O period. The emission reduction percentage is the largest in the BTH region, which may be attributed to the traffic-control measures. Further, we find that the percentage of NO_2 concentration in BJ and TJ still decreases during the Post-O period. This indicates a delay effect of the measures taken to reduce emissions, which positively enhances regional air quality.

Table 5. Statistical values, change rates, and hypothesis test results for the SO_2 concentration (μg/m^3) during the different time periods in the BTH, BJ, TJ, and HB regions based on the historical and current data.

Region	Period	Historical Median	Current Median	Absolute Change	Change Rate	*p* Value
BTH	Pre-O **	13.30	7.44	−5.86	−44.04%	0.000
	O **	10.20	7.25	−2.95	−28.90%	0.000
	Post-O **	8.26	6.94	−1.32	−16.02%	0.000
	Beyond-O	6.77	7.01	0.24	3.58%	0.449
BJ	Pre-O **	3.77	2.61	−1.16	−30.76%	0.000
	O *	3.29	2.68	−0.61	−18.58%	0.013
	Post-O	2.92	2.77	−0.14	−4.88%	0.186
	Beyond-O *	2.67	2.76	0.09	3.20%	0.040
TJ	Pre-O **	10.69	9.18	−1.50	−14.08%	0.001
	O	9.11	8.57	−0.54	−5.91%	0.182
	Post-O *	8.31	8.98	0.67	8.03%	0.014
	Beyond-O **	6.67	8.29	1.62	24.27%	0.000
HB	Pre-O **	16.34	8.53	−7.82	−47.82%	0.000
	O **	11.94	8.10	−3.84	−32.15%	0.000
	Post-O **	9.75	7.72	−2.02	−20.75%	0.000
	Beyond-O	7.87	7.82	−0.04	−0.54%	0.971

*: If $p < 0.05$, the sample is significantly different; **: if $p < 0.01$, the sample is highly significantly different.

Table 6. Statistical values, change rates, and hypothesis test results for the NO_2 concentration (μg/m^3) during the different time periods in the BTH, BJ, TJ, and HB regions based on the historical and current data.

Region	Period	Historical Median	Current Median	Absolute Change	Change Rate	*p* Value
BTH	Pre-O	44.04	41.26	−2.79	−6.33%	0.080
	O *	37.70	29.14	−8.56	−22.70%	0.038
	Post-O **	29.36	23.92	−5.44	−18.52%	0.001
	Beyond-O *	20.56	18.47	−2.09	−10.18%	0.014
BJ	Pre-O	34.48	35.85	1.37	3.97%	0.606
	O **	37.01	24.89	−12.12	−32.74%	0.001
	Post-O **	28.75	21.69	−7.05	−24.53%	0.001
	Beyond-O *	19.70	18.10	−1.60	−8.14%	0.036
TJ	Pre-O *	50.47	43.90	−6.57	−13.02%	0.011
	O	44.51	39.72	−4.79	−10.77%	0.380
	Post-O **	35.24	28.24	−6.99	−19.85%	0.001
	Beyond-O **	24.20	19.06	−5.15	−21.26%	0.001
HB	Pre-O *	45.11	41.57	−3.54	−7.86%	0.031
	O **	35.61	29.93	−5.68	−15.96%	0.006
	Post-O **	28.08	23.35	−4.73	−16.85%	0.001
	Beyond-O	20.55	18.77	−1.78	−8.64%	0.089

*: If $p < 0.05$, the sample is significantly different; **: if $p < 0.01$, the sample is highly significantly different.

The data analysis based on Figure 4f and Table 7 exhibits that O_3 concentrations across the BTH region do not show a significant decrease compared to historical periods.

We further found a negative correlation between NO_2 and O_3 concentrations (a decrease in NO_2 and an increase in O_3 percentage). This change in negative correlation can be attributed to the titration effect in photochemical processes [69]. This titration effect may cause an increase in airborne O_3, which offsets the health benefits due to the reduction in NO_2 [70]. Therefore, while controlling NO_2 emissions, emission-reduction measures would need to control emissions of VOCs simultaneously [31]. Integrating and balancing NO_2 and O_3 emission reductions is the ultimate goal of protecting air quality and people's health.

Table 7. Statistical values, change rates, and hypothesis test results for the O_3 concentration (μg/m^3) during the different time periods in the BTH, BJ, TJ, and HB regions based on the historical and current data.

Region	Period	Historical Median	Current Median	Absolute Change	Change Rate	*p* Value
BTH	Pre-O	28.00	28.46	0.46	1.64%	0.844
	O **	49.99	54.79	4.80	9.59%	0.005
	Post-O	73.51	76.16	2.65	3.61%	0.079
	Beyond-O	104.71	104.37	−0.34	−0.33%	0.080
BJ	Pre-O	31.51	27.50	−4.01	−12.73%	0.510
	O **	44.64	56.46	11.82	26.48%	0.001
	Post-O	68.20	70.91	2.71	3.98%	0.053
	Beyond-O **	92.89	98.33	5.44	5.86%	0.004
TJ	Pre-O	25.42	25.66	0.24	0.95%	0.257
	O *	47.64	51.10	3.46	7.26%	0.040
	Post-O **	64.87	76.46	11.58	17.85%	0.002
	Beyond-O **	98.00	110.54	12.54	12.79%	0.002
HB	Pre-O	29.00	28.65	−0.35	−1.20%	0.794
	O *	52.04	56.16	4.12	7.92%	0.046
	Post-O	75.73	76.63	0.91	1.20%	0.193
	Beyond-O *	104.23	105.22	0.99	0.95%	0.024

*: If $p < 0.05$, the sample is significantly different; **: if $p < 0.01$, the sample is highly significantly different.

3.2. Reduction in Emissions in the BTH Urban Area during the 2022 Winter Olympics

We obtained the percentage changes of criteria air pollutant concentrations across the study area in each city during the Winter Olympic Games (period O) relative to the historical periods, and the statistics of the percentage changes of pollutant concentrations can reflect the strength of the air-control measures enacted in each city.

Figure 5 shows the distribution of the air quality changes for the different types of pollutants during the O period. Among them, the decrease in $PM_{2.5}$ was concentrated in the central (BJ) and northeastern (TJ and QHD) parts of the BTH region, with a decrease of more than 30%, while the concentration in the southern region (XT, HD, and HS) was higher than that during the historical period. The decrease in PM_{10} was concentrated in the northern BTH region (ZJK, CD, and QHD), while the PM_{10} concentration in the northern region was higher than that during the historical period. The CO concentrations in the central and northeastern regions significantly decreased, while the SO_2 concentrations in the westernmost and easternmost regions decreased from historical levels. In addition, the NO_2 concentrations were found to significantly decrease in the northern region while increasing in the southern region, whereas the O_3 concentration in the northern region increased while decreasing in the southern region. Both pollutants caused significant differences between the northern and southern regions. There were significant geographical differences in the changes in the different criteria pollutants relative to the historical periods.

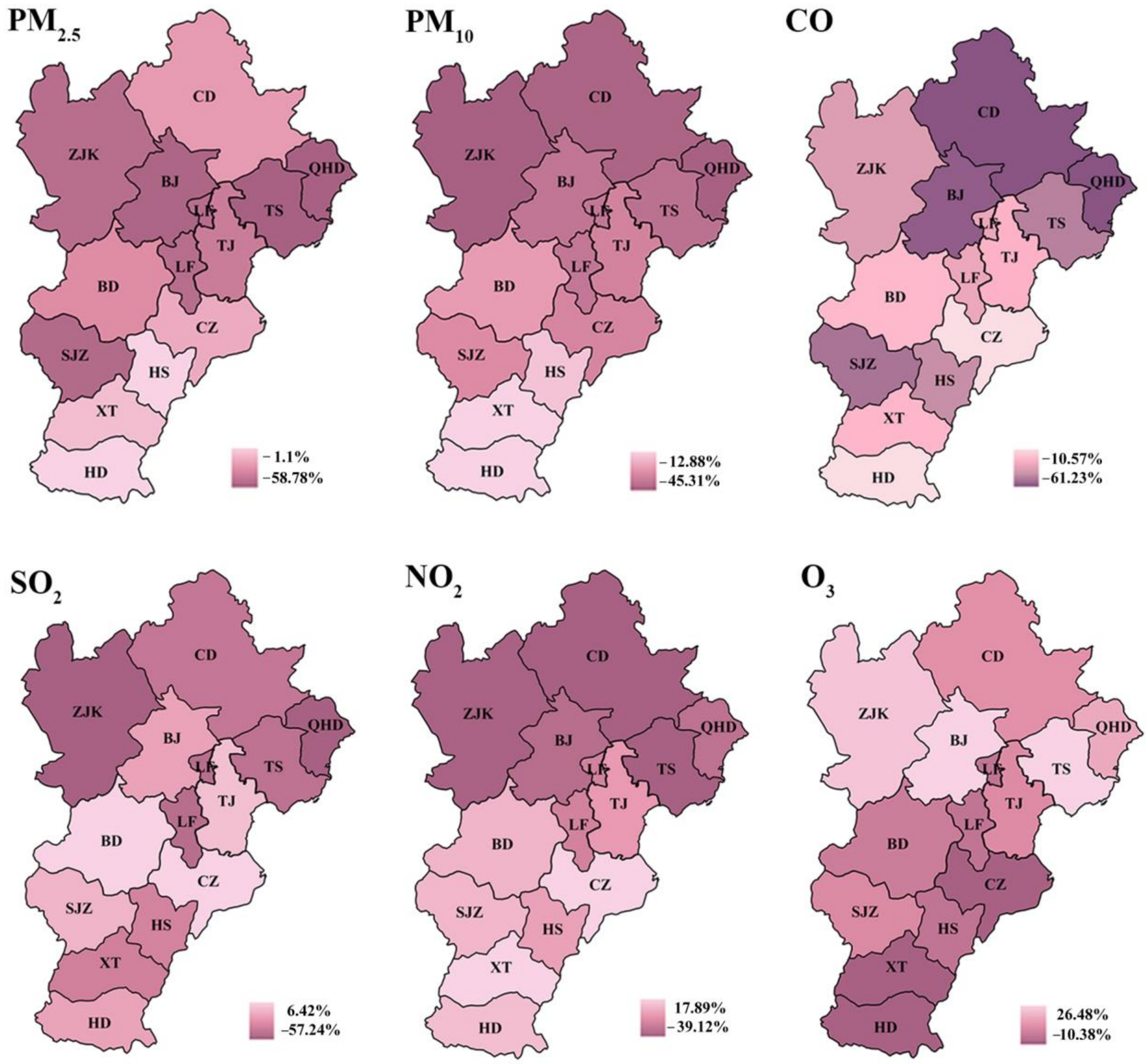

Figure 5. Rate of change of the urban criteria air pollutant concentrations in the study area during the Olympic Games relative to the historical periods, including Beijing (BJ), Tianjin (TJ), Shijiazhuang (SZJ), Tangshan (TS), Qinhuangdao (QHD), Handan (HD), Xingtai (XT), Langfang (LF), Baoding (BD), Hengshui (HS), Zhangjiakou (ZJK), Chengde (CD), and Cangzhou (CZ).

The comprehensive assessment determined that the air pollutant control effect was stronger in the northern part of Beijing, Tianjin, and Hebei than in the southern part. The pollutant concentrations in Zhangjiakou, Chengde, Qinhuangdao, Beijing, and Tangshan were significantly lower than those during the historical periods, which verifies that these areas achieved notable protection during the Winter Olympics.

3.3. Evaluation of the Daily Average Quality via the Air Pollution Concentration in the Cities Hosting the 2022 Winter Olympics

In this section, we evaluate the daily criteria pollutant concentrations in Beijing and Zhangjiakou City, Hebei Province, during the O period to assess the effectiveness of their air control policies directly and effectively and to discern whether the health of personnel was protected during the Olympics. The discussion and analysis of the criteria pollutant concentration exceedance statistics are based on the latest Global Air Quality Guidelines published by the World Health Organization (WHO) in 2021 [71] (Table 8).

Table 8. Global Air Quality Guidelines published by the WHO in 2021 that describe the intermediate targets and air quality guideline (AQG) levels for the different pollutants at different averaging times. The limit values for each pollutant are determined based on their degree of risk to human health, international experience, and the latest scientific research. These limit values can be used as reference standards for government departments and the public to assess and control air pollution.

Items	Averaging Time	Interim Target				AQG Level
		1	2	3	4	
$PM_{2.5}$, μg/m^3	24 h	75	50	37.5	25	15
PM_{10}, μg/m^3	24 h	150	100	75	50	45
O_3, μg/m^3	24 h	100	70	–	–	60
NO_2, μg/m^3	24 h	120	50	–	–	25
SO_2, μg/m^3	24 h	125	50	–	–	40
CO, mg/m^3	24 h	7	–	–	–	4

Interim target: The WHO sets interim targets for various types of emissions, and if these interim targets are met, one can expect the risks of the acute and chronic effects of air pollution on human health to be significantly reduced. Interim target 1 can also be regarded as the maximum value of the emissions of the bound air pollutant. Additionally, this interim target is referred to as the maximum indicator. AQG level: The WHO-recommended emission concentrations of the criteria air pollutants are ultimate goals. At these concentrations, the air pollutants exert a limited impact on human health. Additionally, the AQG level is referred to as the minimum indicator of air pollution emissions.

We calculated the daily average (24 h averaging time) criteria pollutant concentrations in Beijing and Zhangjiakou City during the O period based on the geographical location of the air monitoring stations and the hourly observed concentrations, and the results are shown below (Figure 6). Under the control of relevant air-control measures, the daily average $PM_{2.5}$ concentration in Beijing was below the minimum target (AQG level) on 10 days, exceeded the maximum target (Target 1) on 3 days, and varied between the two targets on the remaining 27 days, while that in Zhangjiakou City was below the minimum target on 8 days and varied between the maximum and minimum targets for the remaining 32 days. The maximum indicator was not exceeded. Therefore, Zhangjiakou City controlled its $PM_{2.5}$ emissions better than Beijing City during the O period. At the same time, the daily average PM_{10} and $PM_{2.5}$ concentration levels at these two locations seemed very similar during this period, and the changes were basically the same.

The statistics showed that the daily average CO and SO_2 concentrations in both areas were below the AQG level, and the safeguard measures played a very positive role in controlling the CO and SO_2 concentrations. In regard to the NO_2 daily average concentration, it was found that the daily average concentration in Zhangjiakou persistently remained below the AQG level, while that in Beijing was below the AQG level on 22 days and varied between the maximum and minimum targets on the remaining 18 days, and the daily average concentrations in both areas did not exceed the maximum emission targets during the O period. Moreover, regarding the O_3 concentration, Beijing exhibited 26 days below the minimum emission index during the O period, while the maximum emission index was not exceeded on the remaining days. In contrast, the level in Zhangjiakou City exceeded the minimum emission index on all days, it exceeded the maximum emission index on two days, and it varied between the maximum and minimum targets on the remaining 38 days. Hence, the control ability of Zhangjiakou City for O_3 was lower than that of Beijing City. Considering the above statistical results, we found that the overall daily average concentrations of the criteria air pollutants were basically lower than the maximum emission reduction limits, the daily average concentration values below the minimum emission reduction limits accounted for the majority of all data, and the overall pollutant concentration control ability of Zhangjiakou was higher than that of Beijing. Therefore, it could be considered that the air-control measures in Zhangjiakou played a more positive role in reducing its pollutant emissions during the Winter Olympics.

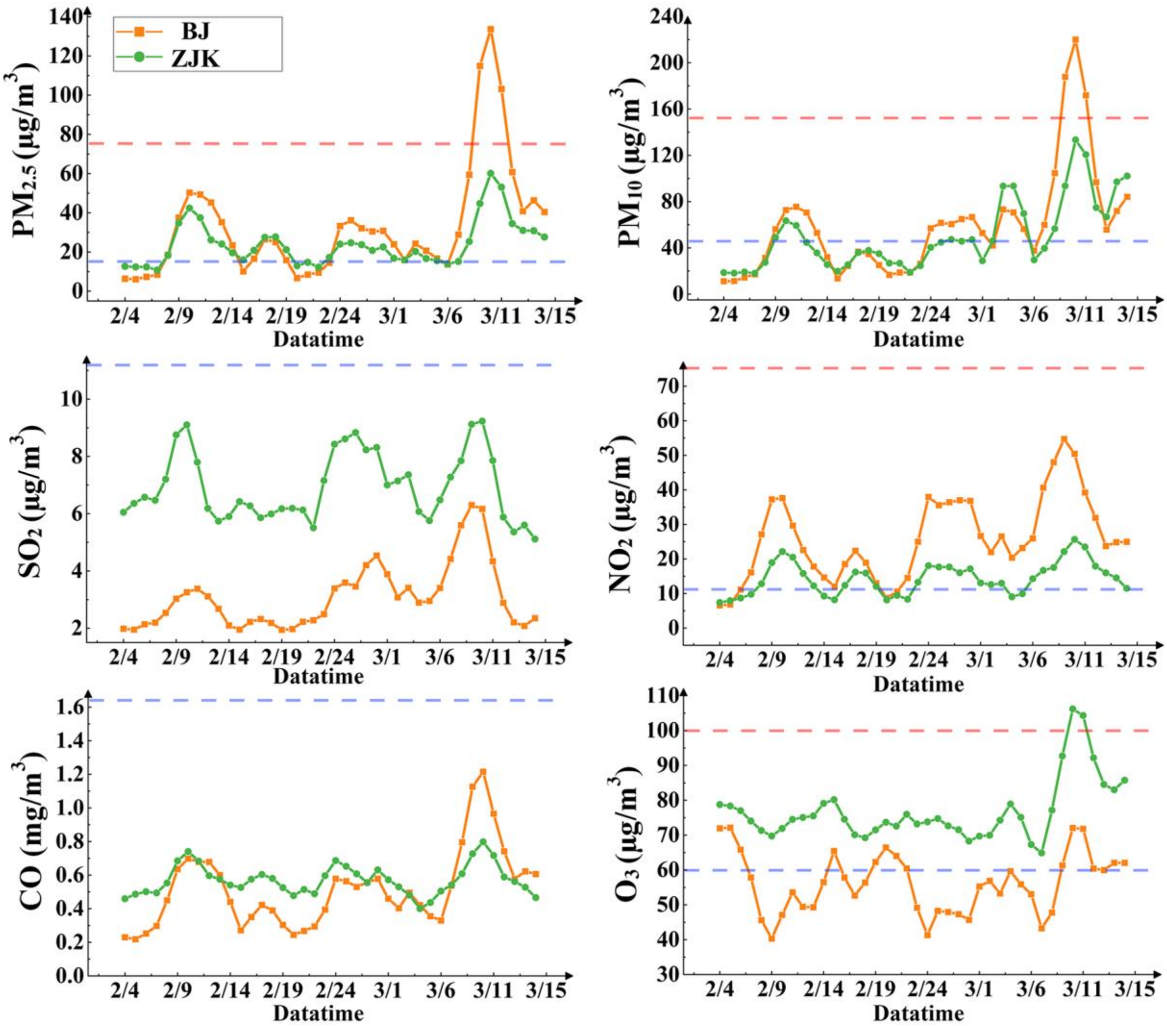

Figure 6. Daily average pollutant concentrations in Beijing (BJ) and Zhangjiakou (ZJK) City during the O period and the WHO urban air criteria pollutant limits. The dotted red line represents Interim target 1; the dotted blue line represents the AQG level concentration value.

4. Conclusions

We used data retrieved from ground–air quality monitoring stations to quantify the concentrations of criteria air pollutants ($PM_{2.5}$, PM_{10}, CO, SO_2, NO_2, and O_3) during the 2022 Winter Olympics and Paralympics in the Beijing, Tianjin, and Hebei regions of China during four periods (Pre-O, O, Post-O, and Beyond-O), thereby comparing their temporal characteristics and spatial differences to those during the historical periods. Moreover, we assessed the concentrations of the criteria air pollutants in Beijing and Zhangjiakou cities based on the Global Air Quality Guidelines published by the WHO and indirectly assessed the effectiveness of the temporary prevention and control policies and regulations implemented by the Chinese government during the Olympic Games (O period). We concluded this based on the following results: (1) Temporal analysis revealed the most substantial decreases in $PM_{2.5}$, PM_{10}, CO, and NO_2 concentrations during the O period. SO_2 experienced its most significant decline in the pre-O period, while O_3 concentrations did not notably decrease compared to historical levels. Notably, $PM_{2.5}$, PM_{10}, and SO_2 concentrations exhibited a lag effect, displaying a significant downward trend during the Post-O period until returning to historical levels in the Beyond-O period. (2) NO_2 and O_3 concentrations exhibit a negative correlation, necessitating emission-reduction strategies to control volatile organic compounds (VOCs) to manage O_3 levels while regulating NO_2 emissions. (3) Variations in industrial structures led to differences in pollutant concentration cycles. Beijing, dominated by high-tech industries, saw significant control during the O period, whereas Hebei and Tianjin, dominated by heavy industries, initiated control during the Pre-O period with a longer cycle. (4) Spatial variations existed among cities: $PM_{2.5}$ concentrations decreased in the central and northeastern parts of the BTH region but increased in the southern region, while PM_{10} and CO concentrations showed diverse patterns across different regions. (5) In the Olympic Games, Zhangjiakou controlled $PM_{2.5}$ better than Beijing, while both cities positively affected CO and SO_2. Zhangjiakou had slightly less control over NO_2 and O_3 compared to Beijing. Despite this, both cities kept daily pollutant levels mostly below set limits, showing the success of the air-control measures during the Olympics. Our study can be used as a reference for enhancing regional atmospheric conditions during significant social events. The research outcomes offer valuable insights for regional environmental decision making, economic development, social governance, and fostering sustainable urban development.

Author Contributions: Z.S.: data curation, formal analysis, investigation, visualization, software, writing—original draft. Z.R.: conceptualization, methodology, supervision, writing—review and editing. J.F.: conceptualization, funding acquisition, methodology, project administration, writing—original draft, writing—review and editing. J.Z.: data curation, investigation, resources, software. Y.G.: visualization, writing—review and editing. F.W.: data curation, investigation, resources, software. All authors have read and agreed to the published version of the manuscript.

Funding: This work was funded by the National Natural Science Foundation of China (Grant No. 42171413), a grant from State Key Laboratory of Resources and Environmental Information System, the Shandong Provincial Natural Science Foundation (Grant No. ZR2020MD015), the National Key Research and Development Program of China (Grant No. 2017YFB0503500), and the Young Teacher Development Support Program of Shandong University of Technology (Grant No. 4072-115016).

Institutional Review Board Statement: Not applicable.

Informed Consent Statement: Not applicable.

Data Availability Statement: Criteria air pollutant concentration data from the study and information on its air monitoring stations are available at the China Environmental Monitoring Center http://www.cnemc.cn (accessed on 10 January 2023).

Acknowledgments: We would like to thank the China National Environmental Monitoring Centre for the hourly surface air criteria pollutant monitoring data. We also appreciate the editors and reviewers for their constructive comments and suggestions.

Conflicts of Interest: The authors declare no conflict of interest.

References

1. Bennett, J.E.; Tamura-Wicks, H.; Parks, R.M.; Burnett, R.T.; Pope, C.A.; Bechle, M.J.; Marshall, J.D.; Danaei, G.; Ezzati, M. Particulate Matter Air Pollution and National and County Life Expectancy Loss in the USA: A Spatiotemporal Analysis. *PLoS Med.* **2019**, *16*, e1002856. [CrossRef] [PubMed]
2. Feng, S.; Gao, D.; Liao, F.; Zhou, F.; Wang, X. The Health Effects of Ambient $PM_{2.5}$ and Potential Mechanisms. *Ecotoxicol. Environ. Saf.* **2016**, *128*, 67–74. [CrossRef] [PubMed]
3. Pui, D.Y.H.; Chen, S.-C.; Zuo, Z. $PM_{2.5}$ in China: Measurements, Sources, Visibility and Health Effects, and Mitigation. *Particuology* **2014**, *13*, 1–26. [CrossRef]
4. Curtis, L.; Rea, W.; Smith-Willis, P.; Fenyves, E.; Pan, Y. Adverse Health Effects of Outdoor Air Pollutants. *Environ. Int.* **2006**, *32*, 815–830. [CrossRef]
5. Greenberg, N.; Carel, R.S.; Derazne, E.; Bibi, H.; Shpriz, M.; Tzur, D.; Portnov, B.A. Different Effects of Long-Term Exposures to SO_2 and NO_2 Air Pollutants on Asthma Severity in Young Adults. *J. Toxicol. Environ. Health A* **2016**, *79*, 342–351. [CrossRef]
6. Pandey, J.S.; Kumar, R.; Devotta, S. Health Risks of NO_2, SPM and SO_2 in Delhi (India). *Atmos. Environ.* **2005**, *39*, 6868–6874. [CrossRef]
7. Nazaroff, W.W.; Weschler, C.J. Cleaning Products and Air Fresheners: Exposure to Primary and Secondary Air Pollutants. *Atmos. Environ.* **2004**, *38*, 2841–2865. [CrossRef]
8. Bozkurt, Z.; Üzmez, Ö.Ö.; Döğeroğlu, T.; Artun, G.; Gaga, E.O. Atmospheric Concentrations of SO_2, NO_2, Ozone and VOCs in Düzce, Turkey Using Passive Air Samplers: Sources, Spatial and Seasonal Variations and Health Risk Estimation. *Atmos. Pollut. Res.* **2018**, *9*, 1146–1156. [CrossRef]

9. Hossain, M.S.; Frey, H.C.; Louie, P.K.K.; Lau, A.K.H. Combined Effects of Increased O_3 and Reduced NO_2 Concentrations on Short-Term Air Pollution Health Risks in Hong Kong. *Environ. Pollut.* **2021**, *270*, 116280. [CrossRef]
10. Tao, C.; Liao, Z.; Hu, M.; Cheng, B.; Diao, G. Can Industrial Restructuring Improve Urban Air Quality?—A Quasi-Experiment in Beijing during the COVID-19 Pandemic. *Atmosphere* **2022**, *13*, 119. [CrossRef]
11. Wang, Y.; Yuan, Y.; Wang, Q.; Liu, C.; Zhi, Q.; Cao, J. Changes in Air Quality Related to the Control of Coronavirus in China: Implications for Traffic and Industrial Emissions. *Sci. Total Environ.* **2020**, *731*, 139133. [CrossRef] [PubMed]
12. Yao, L.; Wang, D.; Fu, Q.; Qiao, L.; Wang, H.; Li, L.; Sun, W.; Li, Q.; Wang, L.; Yang, X.; et al. The Effects of Firework Regulation on Air Quality and Public Health during the Chinese Spring Festival from 2013 to 2017 in a Chinese Megacity. *Environ. Int.* **2019**, *126*, 96–106. [CrossRef] [PubMed]
13. McKenzie, D.C.; Boulet, L.-P. Asthma, Outdoor Air Quality and the Olympic Games. *Can. Med. Assoc. J.* **2008**, *179*, 543–548. [CrossRef] [PubMed]
14. Ventura, L.M.B.; Ramos, M.B.; Santos, J.O.; Gioda, A. Monitoring of Air Quality before the Olympic Games Rio 2016. *An. Acad. Bras. Ciências* **2019**, *91*, e20170984. [CrossRef]
15. Friedman, M.S.; Powell, K.E.; Hutwagner, L.; Graham, L.M.; Teague, W.G. Impact of Changes in Transportation and Commuting Behaviors During the 1996 Summer Olympic Games in Atlanta on Air Quality and Childhood Asthma. *JAMA* **2001**, *285*, 897–905. [CrossRef]
16. Wang, S.; Zhao, M.; Xing, J.; Wu, Y.; Zhou, Y.; Lei, Y.; He, K.; Fu, L.; Hao, J. Quantifying the Air Pollutants Emission Reduction during the 2008 Olympic Games in Beijing. *Environ. Sci. Technol.* **2010**, *44*, 2490–2496. [CrossRef]
17. Ding, J.; van der A, R.J.; Mijling, B.; Levelt, P.F.; Hao, N. NO_x Emission Estimates during the 2014 Youth Olympic Games in Nanjing. *Atmos. Chem. Phys.* **2015**, *15*, 9399–9412. [CrossRef]
18. Li, S.; Xu, S.; Liu, Y. Major Features of China's Current Macro Economy. In *The China Economy Yearbook*; Brill: Leiden, The Netherlands, 2010; Volume 4, pp. 51–61. ISBN 978-90-04-19033-7.
19. Wang, T.; Du, H.; Zhao, Z.; Zhou, Z.; Russo, A.; Xi, H.; Zhang, J.; Zhou, C. Prediction of the Impact of Meteorological Conditions on Air Quality during the 2022 Beijing Winter Olympics. *Sustainability* **2022**, *14*, 4574. [CrossRef]
20. Chu, F.; Gong, C.; Sun, S.; Li, L.; Yang, X.; Zhao, W. Air Pollution Characteristics during the 2022 Beijing Winter Olympics. *Int. J. Environ. Res. Public. Health* **2022**, *19*, 11616. [CrossRef]
21. Wu, Q.; Wu, Z.; Li, S.; Chen, Z. The Impact of the Beijing Winter Olympic Games on Air Quality in the Beijing–Tianjin–Hebei Region: A Quasi-Natural Experiment Study. *Sustainability* **2023**, *15*, 11252. [CrossRef]
22. Central People's Government of the People's Republic of China, Beijing, China. Two Departments on the Beijing-Tianjin-Hebei and Surrounding Areas in the Heating Season of 2021–2022 Steel Industry Peak Production Notice. 2021; p. 1. Available online: http://www.gov.cn/zhengce/zhengceku/2021-10/15/content_5642770.htm (accessed on 30 September 2021).
23. Tianjin Municipal People's Government, Tianjin, China. General Office of Tianjin Municipal People's Government on the Work of the Ban on Fireworks during the Spring Festival in 2022. 5 January 2022. Available online: https://www.tj.gov.cn/zwgk/szfwj/tjsrmzfbgt/202201/t20220110_5775314.html (accessed on 10 January 2022).
24. Beijing Municipal People's Government. Beijing Municipal People's Government Notice on Temporary Traffic Management Measures during the Beijing 2022 Winter Olympic Games and Winter Paralympic Games_Policy Documents_Beijing Municipal People's Government Portal. 2022. Available online: http://www.beijing.gov.cn/zhengce/zhengcefagui/202201/t20220114_2590998.html (accessed on 14 January 2022).
25. Wang, Z.; Li, J.; Liang, L. Spatio-Temporal Evolution of Ozone Pollution and Its Influencing Factors in the Beijing-Tianjin-Hebei Urban Agglomeration. *Environ. Pollut.* **2020**, *256*, 113419. [CrossRef] [PubMed]
26. Lyu, Y.; Ju, Q.; Lv, F.; Feng, J.; Pang, X.; Li, X. Spatiotemporal Variations of Air Pollutants and Ozone Prediction Using Machine Learning Algorithms in the Beijing-Tianjin-Hebei Region from 2014 to 2021. *Environ. Pollut.* **2022**, *306*, 119420. [CrossRef] [PubMed]
27. Huang, R.-J.; Zhang, Y.; Bozzetti, C.; Ho, K.-F.; Cao, J.-J.; Han, Y.; Daellenbach, K.R.; Slowik, J.G.; Platt, S.M.; Canonaco, F.; et al. High Secondary Aerosol Contribution to Particulate Pollution during Haze Events in China. *Nature* **2014**, *514*, 218–222. [CrossRef]
28. Zhu, L.; Gan, Q.; Liu, Y.; Yan, Z. The Impact of Foreign Direct Investment on SO_2 Emissions in the Beijing-Tianjin-Hebei Region: A Spatial Econometric Analysis. *J. Clean. Prod.* **2017**, *166*, 189–196. [CrossRef]
29. Yue, J.; Zhu, H.; Yao, F. Does Industrial Transfer Change the Spatial Structure of CO_2 Emissions?—Evidence from Beijing-Tianjin-Hebei Region in China. *Int. J. Environ. Res. Public Health* **2021**, *19*, 322. [CrossRef]
30. Pei, Z.; Han, G.; Ma, X.; Su, H.; Gong, W. Response of Major Air Pollutants to COVID-19 Lockdowns in China. *Sci. Total Environ.* **2020**, *743*, 140879. [CrossRef]
31. Le, T.; Wang, Y.; Liu, L.; Yang, J.; Yung, Y.L.; Li, G.; Seinfeld, J.H. Unexpected Air Pollution with Marked Emission Reductions during the COVID-19 Outbreak in China. *Science* **2020**, *369*, 702–706. [CrossRef]
32. Zhu, Y.; Xie, J.; Huang, F.; Cao, L. Association between Short-Term Exposure to Air Pollution and COVID-19 Infection: Evidence from China. *Sci. Total Environ.* **2020**, *727*, 138704. [CrossRef]
33. Air Pollution Reduction and Mortality Benefit during the COVID-19 Outbreak in China–The Lancet Planetary Health. Available online: https://www.thelancet.com/journals/lancet/article/PIIS2542-5196(20)30107-8/fulltext (accessed on 12 March 2023).
34. Beelen, R.; Hoek, G.; Cyrys, J.; Eeftens, M.; De Hoogh, K. S-156: Air Pollution Exposure Assessment Using Land Use Regression Modeling in 36 European Study Areas—Results of the ESCAPE Project. *Epidemiology* **2012**, *23*, 1. [CrossRef]

35. Delavar, M.; Gholami, A.; Shiran, G.; Rashidi, Y.; Nakhaeizadeh, G.; Fedra, K.; Hatefi Afshar, S. A Novel Method for Improving Air Pollution Prediction Based on Machine Learning Approaches: A Case Study Applied to the Capital City of Tehran. *ISPRS Int. J. Geo-Inf.* **2019**, *8*, 99. [CrossRef]
36. Gregório, J.; Gouveia-Caridade, C.; Caridade, P.J. Modeling PM2. 5 and PM10 Using a Robust Simplified Linear Regression Machine Learning Algorithm. *Atmosphere* **2022**, *13*, 1334. [CrossRef]
37. Ma, J.; Ding, Y.; Gan, V.J.L.; Lin, C.; Wan, Z. Spatiotemporal Prediction of $PM_{2.5}$ Concentrations at Different Time Granularities Using IDW-BLSTM. *IEEE Access* **2019**, *7*, 107897–107907. [CrossRef]
38. Zheng, M.; Salmon, L.G.; Schauer, J.J.; Zeng, L.; Kiang, C.S.; Zhang, Y.; Cass, G.R. Seasonal Trends in $PM_{2.5}$ Source Contributions in Beijing, China. *Atmos. Environ.* **2005**, *39*, 3967–3976. [CrossRef]
39. D'Amato, G.; Holgate, S.T.; Pawankar, R.; Ledford, D.K.; Cecchi, L.; Al-Ahmad, M.; Al-Enezi, F.; Al-Muhsen, S.; Ansotegui, I.; Baena-Cagnani, C.E.; et al. Meteorological Conditions, Climate Change, New Emerging Factors, and Asthma and Related Allergic Disorders. A Statement of the World Allergy Organization. *World Allergy Organ. J.* **2015**, *8*, 1–52. [CrossRef]
40. Orru, H.; Ebi, K.L.; Forsberg, B. The Interplay of Climate Change and Air Pollution on Health. *Curr. Environ. Health Rep.* **2017**, *4*, 504–513. [CrossRef]
41. Ng, E.; Ren, C. China's Adaptation to Climate & Urban Climatic Changes: A Critical Review. *Urban Clim.* **2018**, *23*, 352–372. [CrossRef]
42. Kinney, P.L. Interactions of Climate Change, Air Pollution, and Human Health. *Curr. Environ. Health Rep.* **2018**, *5*, 179–186. [CrossRef]
43. Wen, W.; Ma, X.; Tang, Y.; Wei, P.; Wang, J.; Guo, C. The Impacts of Meteorology on Source Contributions of Air Pollution in Winter in Beijing, 2015–2017 Changes. *Atmos. Pollut. Res.* **2020**, *11*, 1953–1962. [CrossRef]
44. Pérez, I.A.; García, M.Á.; Sánchez, M.L.; Pardo, N.; Fernández-Duque, B. Key Points in Air Pollution Meteorology. *Int. J. Environ. Res. Public Health* **2020**, *17*, 8349. [CrossRef]
45. Yienger, J.J.; Galanter, M.; Holloway, T.A.; Phadnis, M.J.; Guttikunda, S.K.; Carmichael, G.R.; Moxim, W.J.; Levy, H. The Episodic Nature of Air Pollution Transport from Asia to North America. *J. Geophys. Res. Atmos.* **2000**, *105*, 26931–26945. [CrossRef]
46. Goldman, G.T.; Desikan, A.; Morse, R.; Kalman, C.; MacKinney, T.; Cohan, D.S.; Reed, G.; Parras, J. Assessment of Air Pollution Impacts and Monitoring Data Limitations of a Spring 2019 Chemical Facility Fire. *Environ. Justice* **2022**, *15*, 362–372. [CrossRef]
47. Haryanto, B. Climate Change and Urban Air Pollution Health Impacts in Indonesia. In *Climate Change and Air Pollution*; Springer: Cham, Switzerland, 2018; pp. 215–239. [CrossRef]
48. Yue, X.; Unger, N. Fire Air Pollution Reduces Global Terrestrial Productivity. *Nat. Commun.* **2018**, *9*, 5413. [CrossRef]
49. Shen, L.; Zhao, T.; Wang, H.; Liu, J.; Bai, Y.; Kong, S.; Zheng, H.; Zhu, Y.; Shu, Z. Importance of Meteorology in Air Pollution Events during the City Lockdown for COVID-19 in Hubei Province, Central China. *Sci. Total Environ.* **2021**, *754*, 142227. [CrossRef] [PubMed]
50. Bakar, Z.A.; Mohemad, R.; Ahmad, A.; Deris, M.M. A Comparative Study for Outlier Detection Techniques in Data Mining. In Proceedings of the 2006 IEEE Conference on Cybernetics and Intelligent Systems, Bangkok, Thailand, 7–9 June 2006; pp. 1–6. [CrossRef]
51. Ottosen, T.-B.; Kumar, P. Outlier Detection and Gap Filling Methodologies for Low-Cost Air Quality Measurements. *Environ. Sci. Process. Impacts* **2019**, *21*, 701–713. [CrossRef] [PubMed]
52. Cheng, Z.; Zou, C.; Dong, J. Outlier Detection Using Isolation Forest and Local Outlier Factor. In Proceedings of the Conference on Research in Adaptive and Convergent Systems, Chongqing, China, 24–27 September 2019; pp. 161–168. [CrossRef]
53. Wang, J.; Du, P.; Hao, Y.; Ma, X.; Niu, T.; Yang, W. An Innovative Hybrid Model Based on Outlier Detection and Correction Algorithm and Heuristic Intelligent Optimization Algorithm for Daily Air Quality Index Forecasting. *J. Environ. Manag.* **2020**, *255*, 109855. [CrossRef] [PubMed]
54. Elminir, H.K. Dependence of Urban Air Pollutants on Meteorology. *Sci. Total Environ.* **2005**, *350*, 225–237. [CrossRef] [PubMed]
55. Tasdemir, Y.; Cindoruk, S.S.; Esen, F. Monitoring of Criteria Air Pollutants in Bursa, Turkey. *Environ. Monit. Assess.* **2005**, *110*, 227–241. [CrossRef]
56. de Fatima Andrade, M.; Kumar, P.; de Freitas, E.D.; Ynoue, R.Y.; Martins, J.; Martins, L.D.; Nogueira, T.; Perez-Martinez, P.; de Miranda, R.M.; Albuquerque, T. Air Quality in the Megacity of São Paulo: Evolution over the Last 30 Years and Future Perspectives. *Atmos. Environ.* **2017**, *159*, 66–82. [CrossRef]
57. Xiao, K.; Wang, Y.; Wu, G.; Fu, B.; Zhu, Y. Spatiotemporal Characteristics of Air Pollutants (PM_{10}, $PM_{2.5}$, SO_2, NO_2, O_3, and CO) in the Inland Basin City of Chengdu, Southwest China. *Atmosphere* **2018**, *9*, 74. [CrossRef]
58. Hoque, M.; Ashraf, Z.; Kabir, H.; Sarker, E.; Nasrin, S. Meteorological Influences on Seasonal Variations of Air Pollutants (SO_2, NO_2, O_3, CO, $PM_{2.5}$ and PM_{10}) in the Dhaka Megacity. *Am. J. Pure Appl. Biosci.* **2020**, *2*, 15–23. [CrossRef]
59. Qu, L.; Liu, S.; Ma, L.; Zhang, Z.; Du, J.; Zhou, Y.; Meng, F. Evaluating the Meteorological Normalized $PM_{2.5}$ Trend (2014–2019) in the "2+26" Region of China Using an Ensemble Learning Technique. *Environ. Pollut.* **2020**, *266*, 115346. [CrossRef] [PubMed]
60. Nguyen, G.T.H.; Hoang-Cong, H.; La, L.T. Statistical Analysis for Understanding $PM_{2.5}$ Air Quality and the Impacts of COVID-19 Social Distancing in Several Provinces and Cities in Vietnam. *Water Air Soil Pollut.* **2023**, *234*, 85. [CrossRef] [PubMed]
61. Zhao, X.; Gao, Q.; Sun, M.; Xue, Y.; Ma, R.; Xiao, X.; Ai, B. Statistical Analysis of Spatiotemporal Heterogeneity of the Distribution of Air Quality and Dominant Air Pollutants and the Effect Factors in Qingdao Urban Zones. *Atmosphere* **2018**, *9*, 135. [CrossRef]

62. deSouza, P.; Lu, R.; Kinney, P.; Zheng, S. Exposures to Multiple Air Pollutants While Commuting: Evidence from Zhengzhou, China. *Atmos. Environ.* **2021**, *247*, 118168. [CrossRef]
63. Wang, T.; Song, H.; Wang, F.; Zhai, S.; Han, Z.; Wang, D.; Li, X.; Zhao, H.; Ma, R.; Zhang, G. Hysteretic Effects of Meteorological Conditions and Their Interactions on Particulate Matter in Chinese Cities. *J. Clean. Prod.* **2020**, *274*, 122926. [CrossRef]
64. Gao, J.; Wang, K.; Wang, Y.; Liu, S.; Zhu, C.; Hao, J.; Liu, H.; Hua, S.; Tian, H. Temporal-Spatial Characteristics and Source Apportionment of $PM_{2.5}$ as Well as Its Associated Chemical Species in the Beijing-Tianjin-Hebei Region of China. *Environ. Pollut.* **2018**, *233*, 714–724. [CrossRef]
65. Chang, X.; Wang, S.; Zhao, B.; Xing, J.; Liu, X.; Wei, L.; Song, Y.; Wu, W.; Cai, S.; Zheng, H.; et al. Contributions of Inter-City and Regional Transport to $PM_{2.5}$ Concentrations in the Beijing-Tianjin-Hebei Region and Its Implications on Regional Joint Air Pollution Control. *Sci. Total Environ.* **2019**, *660*, 1191–1200. [CrossRef]
66. Alvarez, R.; Weilenmann, M.; Favez, J.-Y. Evidence of Increased Mass Fraction of NO_2 within Real-World NO_x Emissions of Modern Light Vehicles—Derived from a Reliable Online Measuring Method. *Atmos. Environ.* **2008**, *42*, 4699–4707. [CrossRef]
67. Freedman, B. The ecological effects of pollution, disturbance, and other stresses. In *Environmental Ecology*; Elsevier: Amsterdam, The Netherlands, 1995; pp. 1–10. ISBN 978-0-12-266542-4.
68. Zhao, Y.; Mao, P.; Zhou, Y.; Yang, Y.; Zhang, J.; Wang, S.; Dong, Y.; Xie, F.; Yu, Y.; Li, W. Improved Provincial Emission Inventory and Speciation Profiles of Anthropogenic Non-Methane Volatile Organic Compounds: A Case Study for Jiangsu, China. *Atmos. Chem. Phys.* **2017**, *17*, 7733–7756. [CrossRef]
69. Lee, J.D.; Drysdale, W.S.; Finch, D.P.; Wilde, S.E.; Palmer, P.I. UK Surface NO_2 Levels Dropped by 42% during the COVID-19 Lockdown: Impact on Surface O_3. *Atmos. Chem. Phys.* **2020**, *20*, 15743–15759. [CrossRef]
70. Li, K.; Jacob, D.J.; Liao, H.; Zhu, J.; Shah, V.; Shen, L.; Bates, K.H.; Zhang, Q.; Zhai, S. A Two-Pollutant Strategy for Improving Ozone and Particulate Air Quality in China. *Nat. Geosci.* **2019**, *12*, 906–910. [CrossRef]
71. World Health Organization. *WHO Global Air Quality Guidelines: Particulate Matter (PM2.5 and PM10), Ozone, Nitrogen Dioxide, Sulfur Dioxide and Carbon Monoxide*; World Health Organization: Geneva, Switzerland, 2021; ISBN 92-4-003422-6.